Latin American Journal of Solids and Structures
www.lajss.org

An optimal integrated longitudinal and lateral dynamic controller development for vehicle path tracking

Abstract

In this paper, an optimal controller for integrated longitudinal and lateral closed loop vehicle/driver dynamics proposed to follow desired path in various driving maneuvers, which also improved maneuverability and stability of vehicle over desired path. Designed controller imposed corrected steering angle and torque on the wheels to keep the vehicle on the desired trajectory whilst modified its handling properties. In the next stage, performance of proposed optimal linear quadratic regulator (LQR) controller compared with Proportional-integrated-derivative (PID) one. The proposed controllers has been implemented on vehicle eight degree of freedom model in MATLAB/Simulink. Then the effects of adaptive controller on vehicle path following has been examined for various maneuvers, by driving on the lane change, J-turn, double lane-change and desired tracks. Finally, longitudinal dynamic performance of vehicle has been investigated during severe braking conditions. Simulation results indicated the dominate efficiency of controller on the vehicle stabilization and path following. Also, it improved longitudinal dynamics performance by preventing wheel lock and reducing stopping distance.

Keywords

Vehicle path following; handling; optimal controller; integrated lateral & longitudinal dynamic.

Nematollah Tavan[a*]
Mehdi Tavan[b]
Rana Hosseini[c]

[a,c]Department of Electrical Engineering, Amirkabir University of Technology, Tehran, Iran
[c]r.hosseini.aut@gmail.com
[b]Department of Eletrical Engineering, Islamic Azad University, Mahmudabad branch, Mahmudabad, Iran
[b]M.tavan@srbiau.ac.ir

Corresponding author:
[a*]jam.tavan@yahoo.com

http://dx.doi.org/10.1590/1679-78251365

Received 20.05.2014
In revised form 22.08.2014
Accepted 13.10.2014
Available online 11.11.2014

1 INTRODUCTION

In the last decade, important researches have been undertaken to improve safety driving and reducing accidents. Consequently considerable attention has been given to the development of the stability and steerability control systems such as electronic stability program (ESP), different active steering, and active braking control systems. An important issue for the chassis control systems is to control the lateral vehicle motion variables such as the yaw rate and side-slip angle by controlling the vehicle yaw moment. Active steering systems in front (AFS) or both in front

and rear (4WS) can effectively improve the steerability performance in the linear region of the tire (Hwang et al., 2008; Jinlai et al., 2011). Kang et al. (2008) investigated the steering controller for path-tracking and a speed controller for improving the safety of lateral vehicle behavior. In critical high lateral acceleration situations that the tire is in nonlinear region, however, a direct yaw moment control (DYC) system can make the vehicle stable (Shuai et al., 2014; Mashadi et al., 2014; Yamakado, 2012).

Tchamna and Youn (2013) presented a new approach for controlling the yaw rate and side-slip of a vehicle without neglecting its longitudinal dynamics and without making simplifying assumptions about its motion. A sliding-mode controller is used to develop a differential braking controller for tracking a desired vehicle yaw rate for a given steering wheel angle, while keeping the vehicle's side-slip angle as small as posible. Kazemi et al. (2000) presented a new method for finding slip control law of Anti-lock Braking System (ABS), based on sliding mode control method. A four wheel vehicle model with seven degrees of freedom were considered. Slip of each wheel controlled separately so that it remained in the desired range for every kind of road condition, and by tuning desired slip undesired yaw on miu-split surfaces has been prevented. One of the adverse effects of sliding mode approaches are high-frequency fluctuations. An optimization-based braking pressure control laws for the front and rear wheels were analytically designed based on a nonlinear two-axle vehicle model (Mirzaeinejad and Mirzaei, 2010b). The integral feedback technique was also appended to the design method to increase the robustness of the controller in the presence of modelling uncertainties. Mashadi et al. (2013) developed the optimal path following controller based on genetic algorithm for lateral dynamics of vehicle. Simulation results demonstrated that the proposed controller was able to effectively keep the vehicle path appropriately close to the desired path even in the presence of the driver commands. The main objective of this paper is designing optimal controller of integrated lateral/longitudinal vehicle dynamics based on controlling combined slips to improve vehicle handling properties and tracking desired path.

The vehicle path control and handling improvement is treated by Yang et al. (2009); Horiuchi et al. (1999) respectively. They used integrated AFS and DYC systems by application of nonlinear predictive control. The AFS was used in low lateral accelerations and the DYC for high-g maneuvers wherein the tires were saturated and couldn't produce enough lateral forces to control the vehicle on the path. This combination showed that the vehicle maneuverability and stability can be remarkably improved. Mashadi et al. (2014) proposed a GA-PID controller with optimized gains for the control of integrated driver/DYC system. Doumiati et al. (2013) investigated the coordination of active front steering and rear braking in a driver-assist system for vehicle yaw control by using robust $H\infty$ approach. A fuzzy method to control ESP and AFS proposed in (Chu et al., 2012). They applied genetic algorithm to optimize the control rule to ensure the correctness and accuracy of the control rule.

It has been shown that DYC is the most effective method on vehicle motion control compared with the other conventional control systems such as four wheel steering (4WS) (Abe, 1999; Selby et al., 2001). The 4WS control, which depends on the relation between tire lateral force and the steer angle as a control command, is efficient in a range where the lateral acceleration is low. But, in high lateral accelerations, the steer input loses its direct effectiveness on tire lateral force and thus on the yaw moment. Therefore, the lateral dynamics parameters, yaw rate and side-slip angle, can no longer be controlled by the steer command.

In previous works, regardless of simultaneous lateral and longitudinal vehicle dynamic modeling system, controller with fewer degrees of freedom has been used to path following or improving handling conditions (Mahmoodi et al., 2013; Mokhiamar and Abe, 2002; Mirzaeinejad and Mirzaei, 2010a; Mashadi and Majidi, 2014). Various control methods such as sliding mode, PID, optimal LQR, and fuzzy approaches for vehicle dynamics control has been used in references frequently (Zhangand et al., 2009; Silva and Sousa, 2011; Guo et al., 2013). Wu et al. (2010) proposed a new integrated robust model based on $H\infty$ controller matching chassis controller to improve vehicle handling performance and lane keep ability. In order to evaluate the effectiveness of controller vehicle lane keeping and stability is tested by a closed loop driver/vehicle model under a transverse forces.

In this paper for a suitable desired model for vehicle handling, combined lateral and longitudinal vehicle dynamics are developed to be tracked by integrated AFS/DYC control system. Firstly, an optimal LQR and PID controller are designed for improving stability, maneuverability and path following of comprehensive vehicle model. Then, considering some admissible tracking errors, an optimal yaw moment control law is developed to reduce the external yaw moment as much as possible by adequately following the desired path and improving its handling properties. An optimal problem is formulated to track the proposed comprehensive vehicle model for yaw rate, side-slip angle and longitudinal slip. Longitudinal dynamic of the vehicle is controlled with the throttle/brake pedal and longitudinal slip. Also, the lateral dynamic, side slip angle and yaw rates are controlled through integrated AFS/DYC system. Therefore, according to the road profile and vehicle location, vehicle tracks the desired path with minimal lateral deviation and heading angle error.

2 VEHICLE MODELLING

In this article, to simulate the control of a vehicle during the path following at various maneuvers, a non-linear 8-DOF vehicle model that includes both lateral and longitudinal dynamics is used. A schematic of typical front wheel steering passenger car is illustrated in Figure 1. The DOFs associated with this model are the longitudinal velocity u, the lateral velocity v_y, the yaw rate r, the roll rate $\dot{\Phi}$, and four wheel rotational speeds, w_{fl}, w_{fr}, w_{rl} and w_{rr}. Sources of nonlinearity includes nonlinear behavior of tires, nonlinearities exist in the longitudinal and the lateral tire normal load transfers, the roll steer effects, and the camber angle changes due to the vehicle roll.

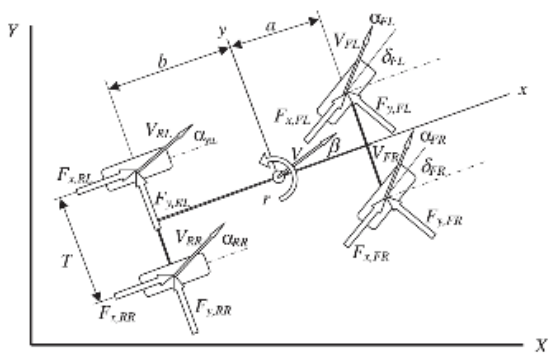

Figure 1: Vehicle 8 dof model (Mahmoodi et al., 2013).

The governing equation of longitudinal dynamic, the lateral motion (lateral velocity, yaw rate and roll angle) are given as follows respectively:

$$M(\dot{u} - rv) = \sum F_x \tag{1}$$

$$M(\dot{v} + ru) + m_s h_s \ddot{\Phi} = \sum_{i=1}^{4} F_y \tag{2}$$

$$I_{zz}\dot{r} - I_{xz}\ddot{\Phi} = \sum M_z \tag{3}$$

$$I_{xx}\ddot{\Phi} - I_{xz}\dot{r} = \sum M_x \tag{4}$$

where M and m_s are the total mass and the rolling mass respectively, I_{zz} and I_{xx} are mass moment of inertia about z-axis and x-axis, I_{xz} is the product of inertia with respect to x and z axes. h_s is the height of sprung mass CG to roll axis. The terms $\sum F_x$ and $\sum F_y$ are external forces along the x and y directions and $\sum M_x$ and $\sum M_z$ are the sums of the moments acting around the roll and yaw axes of the vehicle-fixed coordinate system and can be evaluated from:

$$\sum F_x = F_{xfl} + F_{xfr} + F_{xrl} + F_{xrr} \tag{5}$$

$$\sum F_y = F_{yfl} + F_{yrl} + F_{yrl} + F_{yrr} \tag{6}$$

$$\sum M_z = a(F_{yfl} + F_{yfr}) - b(F_{yrl} + F_{yrr}) + \frac{T}{2}[(F_{xfl} + F_{xrl}) - (F_{xfr} + F_{xrr})] + \sum_{i=1}^{4} M_{zi} \tag{7}$$

$$\sum M_x = -m_s h(\dot{v} + ru) + (m_s gh - k_\Phi)\Phi - C_\Phi \dot{\Phi} \tag{8}$$

In the above equations, a and b are respectively the distances measured from the CG to the front and the rear axles. T is the track width, and K_Φ and C_Φ are the overall roll stiffness and the damping coefficient respectively.

External forces $\sum F_x$ and $\sum F_y$, can be related to the tractive and the lateral tire forces through below equations:

$$F_{xi} = F_{li}\cos\delta_i - F_{li}\sin\delta_i \qquad \text{with} \quad i = fl, fr, rl, rr \tag{9}$$

$$F_{yi} = F_{li}\cos\delta_i + F_{ri}\sin\delta_i \qquad \text{with} \quad i = fl, fr, rl, rr \tag{10}$$

Given that the Vehicle is the front wheel steering, steering angle (δ_i) can be considered as:

$$\delta_{fl} = \delta_{fr} = \delta_f + \Delta\delta_{fl} + K_{rsf}\Phi \tag{11}$$

$$\delta_{rl} = \delta_{rr} = K_{rsr}\Phi \tag{12}$$

In the equations (11) and (12), K_{rsf} and K_{rsr} are steer by roll coefficient for the front and rear wheels which depend on suspension geometry.

2.1 Tyre model

In this paper the mathematical model proposed by Fiala (1954), is used to the analysis of lateral force due to side slip of the tire. It is commonly called Fiala's theory and is related to the tire cornering characteristics which takes into account the interactions between longitudinal and side forces as:

$$F_y = \begin{cases} u\left|F_z\right|\mathrm{sgn}(\alpha) & \alpha \geq \alpha_{cr} \\ u\left|F_z\right|\mathrm{sgn}(\alpha)(1-H^3) & \alpha \leq \alpha_{cr} \end{cases} \tag{13}$$

$$u = u_{\max} - (u_{\max} - u_{\min})S_{s\alpha} \tag{14}$$

$$S_{s\alpha} = \sqrt{S_S^2 + \tan^2\alpha} \tag{15}$$

$$\alpha_{cr} = \tan^{-1}\left(\frac{3u\left|F_z\right|}{C_\alpha}\right) \tag{16}$$

$$H = 1 - \frac{C_\alpha\left|\tan\alpha\right|}{3u\left|F_z\right|} \tag{17}$$

where, a, S_s, S_{sa} are side slip angle, Longitudinal slip ratio the comprehensive slip ratio respectively. Lateral side slip angle for front (a_f) and rear tires (a_r) are given as:

$$\alpha_f = \delta - \tan^{-1}\left(\frac{\nu + ar}{u}\right) \tag{18}$$

$$\alpha_r = -\left(\frac{\nu - br}{u}\right) \tag{19}$$

According to integrated lateral/longitudinal dynamic of vehicle, vertical tire loads on wheels can be expressed as:

$$F_{z1} = \frac{mg}{2}\left\{\frac{b}{l} - \frac{a_x}{g}\left(\frac{h}{l}\right) + K_R\left[\frac{a_{ys}}{g}\left(\frac{h}{T}\right) - \left(\frac{m_s}{m}\right)\left(\frac{h_s}{T}\right)\sin\Phi\right]\right\} \tag{20}$$

$$F_{z2} = \frac{mg}{2}\left\{\frac{a}{l} + \frac{a_x}{g}\left(\frac{h}{l}\right) + (1-K_R)\left[\frac{a_{ys}}{g}\left(\frac{h}{T}\right) - \left(\frac{m_s}{m}\right)\left(\frac{h_s}{T}\right)\sin\Phi\right]\right\} \tag{21}$$

$$F_{z3} = \frac{mg}{2}\left\{\frac{b}{l} - \frac{a_x}{g}\left(\frac{h}{l}\right) - K_R\left[\frac{a_{ys}}{g}\left(\frac{h}{T}\right) - \left(\frac{m_s}{m}\right)\left(\frac{h_s}{T}\right)\sin\Phi\right]\right\} \tag{22}$$

$$F_{z4} = \frac{mg}{2}\left\{\frac{a}{l} + \frac{a_x}{g}\left(\frac{h}{l}\right) - (1-K_R)\left[\frac{a_{ys}}{g}\left(\frac{h}{T}\right) - \left(\frac{m_s}{m}\right)\left(\frac{h_s}{T}\right)\sin\Phi\right]\right\} \tag{23}$$

where a_x and a_y are longitudinal and lateral acceleration respectively. K_R is the ratio of the front roll stiffness to the total roll stiffness which determines the front/rear distribution of total lateral load transfer, and h denotes the height of CG relative to the ground.

2.2 Closed loop vehicle model

In order to realize the simulation results, a driver model utilized in closed loop vehicle model, for the purpose of developing and testing of vehicle stability.

There is a general consensus that in driver model control occurs at two levels (Gordon et al., 2002; Moon and Choi, 2011): preview control (open loop feedforward), in which the driver anticipates the path ahead and makes an appropriate steering action based on knowledge of the vehicle dynamics; and compensatory control (closed-loop feedback), in which the driver compensates for errors in the preview control and for disturbances. The compensatory task involves the human operator controlling a system to minimize an error.

It has been shown that the proposed integrated human drive model can control a vehicle in the same way human manual driving does in various road curvature situations. It can also represent a normal driver's driving motion. Consequently, the integrated human driver model presented in this study can be used into a closed-loop simulation and for the development of a vehicle's intelligent safety system.

One popular method is treating the human control behavior as a linear continuous feedback control, and expressing it as a transfer function. Various transfer functions have then been proposed to suit different conditions. Here, the following transfer function is used (Abe, 2004):

$$H(s) = h\left(\tau_D S + 1 + \frac{1}{\tau_I S}\right) e^{-\tau_L S} \tag{24}$$

Firstly, a driver will have a time delay to decide and make an action. This is represented by $e^{-\tau_L}$; and the time lag is expressed by τ_L; Certain time delay between the driver's perception and reaction exits which ranging from 0.1-0.5s. In the proposed driver model ion this paper time delay has been selected 0.3 seconds.

The control action that the human operator can do includes proportional (h), derivative (τ_D) and integrated (τ_I) control actions to regulate the driver commands based on inputs. In other words, the vehicle driver, in general is considered as both the compensator and the estimator, with certain time delay, in a common closed-loop control system.

3 CONTROLLER DESIGN

The purpose of control system proposed in this paper is controlling the vehicle to follow a desired path, whereas maintains the vehicle actual motions, yaw rate and slip angles, close to their desired responses with a minimum external yaw moment, for improving vehicle stability and handling condition. To achieve this aim, an optimal LQR and PID approaches should be applied for development of the yaw moment and steering angle control law. The control system is under consideration here is shown in Fig. 2.

At the first step in the design of driver/vehicle controller, one should develop an integrated lateral/longitudinal vehicle dynamic model, which is a good representation of the comprehensive vehicle dynamics, for steady state vehicle handling property analysis. The standard form of this model can be found throughout the literature, such as (Mashadi et al., 2014; Vahedi et al., 2011).

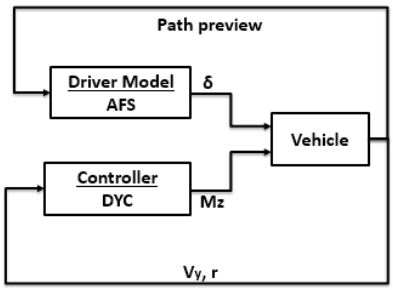

Figure 2: Schematic of Control law procedure.

Despite to control the vehicle in desired path, relationship between the vehicle and the intended path identified by expressing in terms of a lateral position error, y_e (the lateral distance between the vehicle and the intended path), and an orientation angle error ($\psi_v - \psi_r$). The lateral deviation (y_e) and heading error (ψ) of the vehicle are computed by augmenting this model with vehicle variables as:

$$\dot{y}_e = u\sin(\psi) + v\cos(\psi) \tag{25}$$

$$\dot{\psi} = \dot{\psi}_v - \dot{\psi}_r \tag{26}$$

where indexes v and r are representative of vehicle and road respectively and $\dot{\psi}_r$ is defined as road curvature rate which equals longitudinal velocity divided by road curvature, (u/R).

Combining of vehicle model equations with external yaw moment and equations (25) and (26) can be described by the following state space equations based on small heading angle error and constant longitudinal vehicle speed assumptions:

$$\dot{X} = AX + E\delta + BM_z + K\left(1/R\right) \tag{27}$$

$$X = \begin{bmatrix} y_e \\ \nu \\ \psi \\ r \end{bmatrix} \quad A = \begin{bmatrix} 0 & 1 & u & 0 \\ 0 & a_{11} & 0 & a_{12} \\ 0 & 0 & 0 & 1 \\ 0 & a_{21} & 0 & a_{22} \end{bmatrix} \quad E = \begin{bmatrix} 0 \\ e_1 \\ 0 \\ e_2 \end{bmatrix} \quad B = \begin{bmatrix} 0 \\ 0 \\ 0 \\ b \end{bmatrix} \quad K = \begin{bmatrix} 0 \\ 0 \\ -u \\ 0 \end{bmatrix} \tag{28}$$

where,

$$\begin{cases} a_{11} = -2\dfrac{C_{\alpha f} + C_{\alpha r}}{Mu}, \quad a_{12} = 2\dfrac{bC_{\alpha r} - aC_{\alpha f}}{Mu} - U, \quad a_{21} = 2\dfrac{bC_{\alpha r} - aC_{\alpha f}}{I_z u} \\ a_{22} = -2\dfrac{a^2C_{\alpha f} + b^2C_{\alpha r}}{I_z u}, \quad e_1 = 2\dfrac{C_{\alpha f}}{M}, \quad e_2 = -2\dfrac{aC_{\alpha f}}{I_z}, \quad b = \dfrac{1}{I_z} \end{cases}$$

For the vehicle model, the lateral velocity v and the yaw rate r are considered as the two state variables while the yaw moment M_z is the control input, which must be calculated through the control law. Furthermore, the vehicle steering angle δ is considered as the external disturbance which controlled by driver model that should be added to vehicle model states through driver model.

In order to develop the yaw moment control law for improving vehicle handling properties, the linear quadratic regulator (LQR) method is considered here as a suitable tool. In order to comparison controller law effects, PID controller applied to achieve compare with LQR method.

3.1 Optimal LQR controller

To control a vehicle to track a driver intended path with constant longitudinal velocity thereby LQR theory, the performance index that penalizes the tracking errors and control expenditure is formulated as:

$$J = 1/2\int_{t_0}^{t_f}\left[w_1\left(y_e - y_{ed}\right)^2 + w_2\left(\psi - \psi_d\right)^2 + w_3\left(\nu - \nu_d\right)^2 + w_4\left(r - r_d\right) + w_5\left(\delta - \delta_d\right)^2 + w_6 M_z^2\right]\mathrm{d}t \quad (29)$$

where, M_z denotes external yaw moment. The subscript d denotes the desired response of each variable. First and second terms in the performance index are lateral deviation and heading error, which are representations of vehicle path following. Third and fourth term in performance index denote handling and stability property of vehicle and fifth term is vehicle steering angle which regulated by driver. $w_1 - w_6$ are weighting factors which indicate the relative importance of the corresponding terms.

The typically defined optimal control consists of the state variable feedback signal and the disturbance feedforward signal that is related to the road specification, are expressed as:

$$M_z = K_\upsilon \upsilon + K_r r + K_\psi \psi + K_\delta \delta + K_{\dot{\delta}} \dot{\delta} + K_{y_e} y_e + K_R R \quad (30)$$

K_υ, K_r, K_ψ, K_δ, $K_{\dot{\delta}}$, K_{y_e} are known as the state gains of lateral velocity, yaw rate, heading angle, steering angle, steering angle rate, and lateral displacement respectively, which act on the vehicle states and K_R is the preview gain, acting on the previewed path information.

Consequently, equation (29) can be rewritten in the standard form of the optimal control as:

$$J(u) = \frac{1}{2}\int_0^\infty \left[U^T R U + \left(X_d - X\right)^T Q\left(X_d - X\right)^2\right]\mathrm{d}t \quad (31)$$

where X_d is the desired values that the vehicle states should track, Q is a positive semi-definite state weighting matrix, and R the positive semi-definite control weighting matrix. In order to solve the LQR problem the Hamiltonian function can have the following form:

$$H = 1/2\left[(X - X_d)^T Q(X - X_d) + U^T R U + P^T(AX + BU + EW)\right] \quad (32)$$

where P_T is the Lagrange multipliers vector can be written as:

$$P(t) = \left[P_1, P_2, P_3, P_4, P_5, P_6\right]^T \quad (33)$$

Following the general approach of a typical optimal control problem, the following equations, as the necessary conditions, must be satisfied:

$$\begin{cases} \dot{X} = \dfrac{\partial H}{\partial P} = AX + BU + EW \\ \dot{P} = -\dfrac{\partial H}{\partial X} = -Q(X - X_d) - A^T P \\ 0 = \dfrac{\partial H}{\partial U} = RU + B^T P \end{cases} \tag{34}$$

Now suppose that the Lagrange multipliers can be written in the following form:

$$P = KX + S \tag{35}$$

where K is symmetric matrix of feedback gains and S represents feedforward gains matrix. Hence controller input can be written as:

$$U = -R^{-1}B^T(KX + S) \tag{36}$$

Combining equations (32), (34) and (35) lead to

$$\dot{K}X + K\dot{X} + \dot{S} = -Q(X - X_d) - A^T P \tag{37}$$

Time varying gains cause complication and the divergence in solutions. Also, these values converge rapidly to constant values. Therefore, this variable is ignored ($\dot{K} = \dot{S} = 0$). This leads to

$$\begin{cases} KA + A^T K + Q - KBR^{-1}B^T K = 0 \\ \left[A^T - KBR^{-1}B^T\right]S - QX_d + KFW = 0 \end{cases} \tag{38}$$

The first equation in equation (19) is known as the Riccatti equation. The solution for this equation will determine the elements of K and can be solved numerically (Kirk, 2004; Goodarzi et al., 2006) by using MATLAB software. Substituting K into the second equation of equation (19) and solving for S

$$S = -\left[A^T - KBR^{-1}B^T\right]^{-1} KFW \tag{39}$$

With the matrices S and K and substituting in equation (36), and then the controller input can be determined as:

$$M_z = \frac{1}{I_z w_1}\left[K_{41}y_{de} + K_{42}\dot{y}_{de} + K_{43}\psi + K_{44}\dot{\psi} + K_{45}\delta + K_{46}\dot{\delta} + K_{Road}\left(1/R\right)\right] \tag{40}$$

Values of the state gains are set up based on time variation, in such a way that the optimal controller is able to control the vehicle's track and stability. It results in minimum lateral deviation and obtaining vehicle stability and maneuverability over various paths. Their variation in different range of vehicle longitudinal speed are illustrated in Figs. 3.

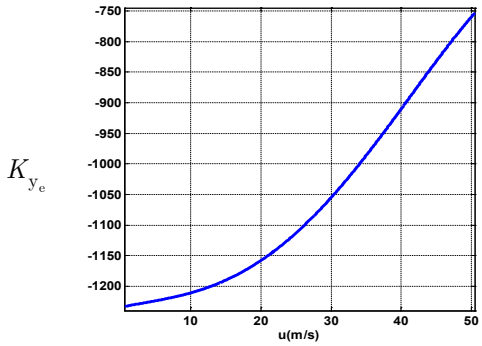

Lateral deviation feedback

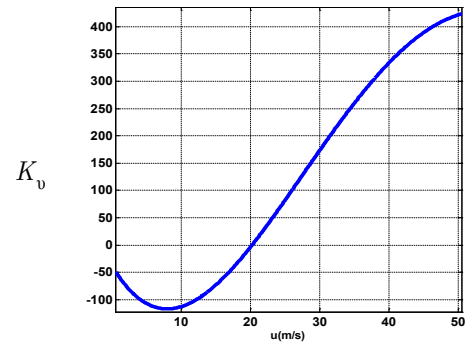

Lateral speed feedback

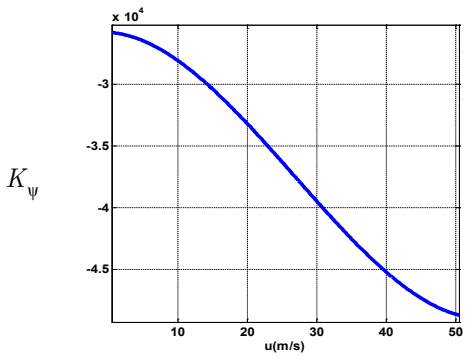

Heading angle feedback

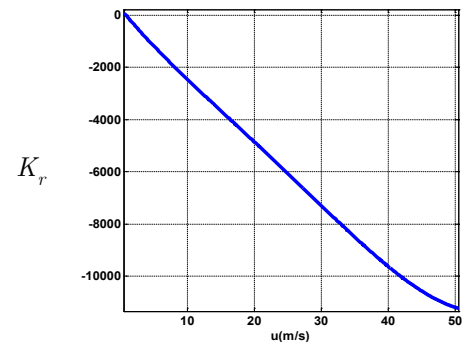

Yaw rate feedback

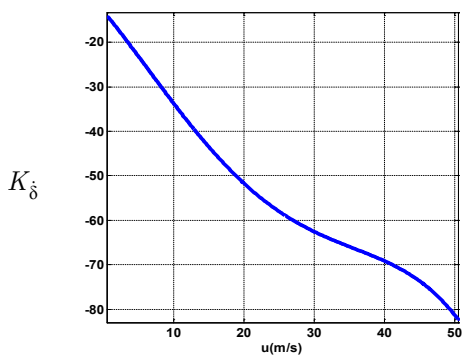

Steering angle rate feedback

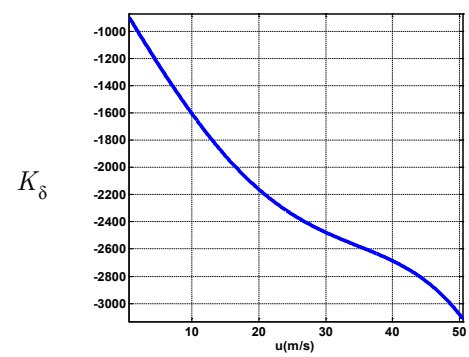

Steering angle feedback

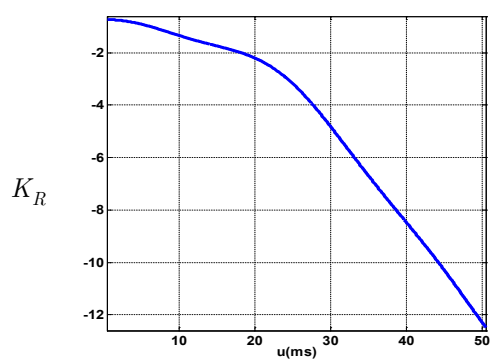

Road radius feedforward

Figure 3: Feedforward and feedback state gains (lateral speed, lateral deviation, yaw rate, heading angle, steering angle, steering angle derivative, and road radius) versus longitudinal speed (m/s).

3.2 PID controller

The PID controller is based on simple ideas. As illustrated in Fig. 4, the idealized formula the transfer function of a PID controller is described as equation (41), which, the controller output is a combination of three terms:

- The proportional term acts to current errors.
- Past errors are accounted for by the integral term.
- The derivative term anticipates future errors by linear extrapolation of the error.

$$G_c(s) = k_p + \frac{k_i}{s} + k_d s \tag{41}$$

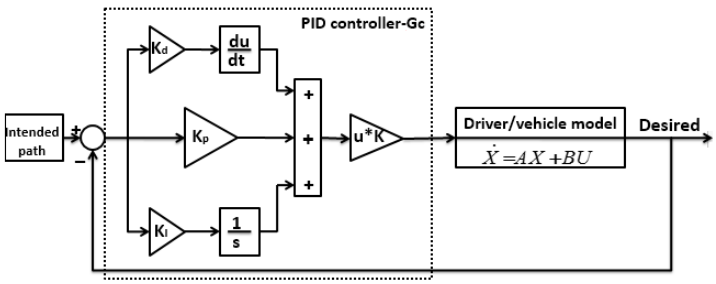

Figure 4: PID controller acting on closed loop vehicle.

A proportional controller (K_p) will have the effect of reducing the rise time and will reduce but never eliminate the steady-state error. An integral control (K_i) will have the effect of eliminating the steady-state error for a constant or step input, but it may make the transient response slower. A derivative control (K_d) will have the effect of increasing the stability of the system, reducing the overshoot, and improving the transient response. Note that these correlations may not be exactly accurate, because K_p, K_i, and K_d are dependent on each other. In fact, changing one of these variables can change the effect of the other two. For this reason, tradeoff between control gains has been performed. In this study the method used to tune the PID controller was the poles allocation (Alonso, 2013; Cominos and Munro, 2002). In the design of the PID controller, the study is based on the performance index of these:

(1) Settling time less than 2s, within 1% of final value;
(2) Overshot of step responsive less than 10%;
(3) Steady-state error of step responsive is 0.

4 SIMULATION RESULTS

Simulation has been performed for both vehicle longitudinal and lateral dynamics with PID, Optimal LQR and without controllers. Simulations were run in Matlab/Simulink software. In the first step, vehicle longitudinal dynamic performance during braking has been compared for three cases. Then in the next stage, vehicle path following over various maneuvers has been investigated with and without controllers. Then vehicle handling properties analyzed for lane change maneuver. Finally, vehicle obstacle avoidance by previewing path has been compared for PID and LQR controllers.

4.1 Longitudinal dynamic results

In order to investigate the effects of controller on vehicle longitudinal dynamic, stopping distance and braking force on tire are compared for uncontrolled, PID and optimal LQR controllers in Figs. 5 respectively.

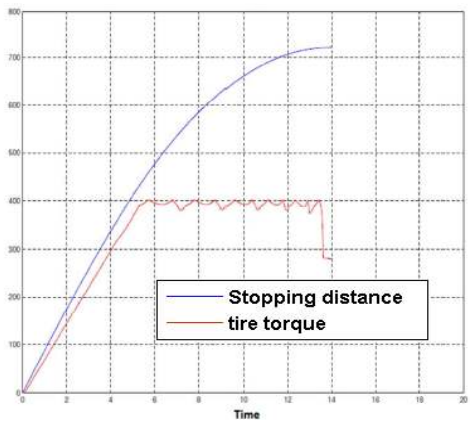

(a) Optimal LQR controller

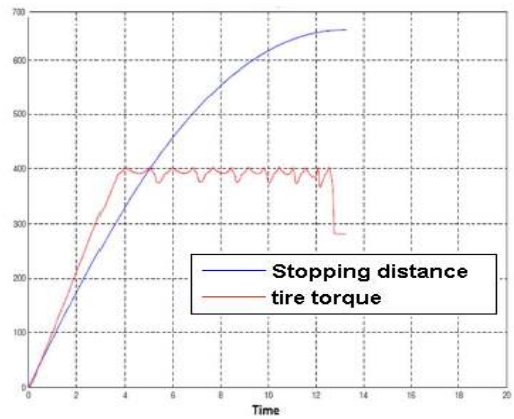

(b) PID controller

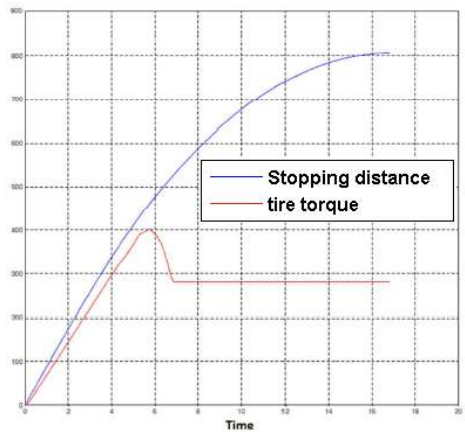

(c) Without controller

Figure 5: Stopping distance and tire lateral force comparison for (a) optimal LQR controller, (b) PID controller and (c) without controller.

Results reveal that forces act on tire in uncontrolled mode, proportional to the longitudinal tire slip are less. Therefore, road holding and steerability of vehicle reduce. Whereas, in controlled modes, tire slip limited in sufficient range which result in improving maneuverability and reducing stooping distance (time). Also, Figure 5 depicts that optimal controller has the minimum time to stop and best performance.

In the next stage for a closer look at the vehicle's steerability, wheel and vehicle speeds variation during braking are compared for three above mentioned conditions in Fig. 6. It can be observed without controller, after 10 seconds of braking, wheel speed becomes zero while the vehicle stops after 17 seconds. In other words, in uncontrolled mode, the wheel locked after 10 seconds

and steerability drastically reduced. However with the addition of controllers, vehicle and wheel speeds simultaneously reached zero, and wheel locking mode didn't occur. Also, results in table 6 indicate that stopping time and distance are less for optimal LQR controller in comparison to PID one.

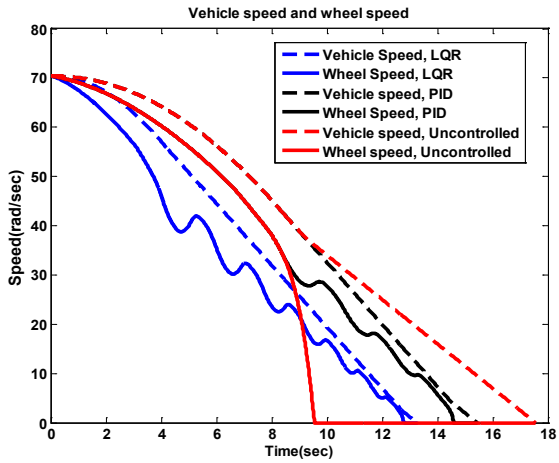

Figure 6: Speed variation during braking for uncontrolled, PID and optimal LQR controllers.

Control strategy	LQR	PID	Without control
tire locking time	-	1 sec	7 sec
stopping	13 sec	15 sec	17 sec
Longitudinal slip	0.2	0.2	7

Table 1: Comparison of vehicle longitudinal performance.

The simulation results indicate that, the wheel slip tracking error is remarkably decreased by the proposed controller. Moreover, the achieved control input is entirely smooth and suitable for implementation, which prevents from wheel locking and steerability losing.

4.2 Lateral dynamics simulation results

Vehicle simulation results has been performed over different paths: quadratic, lanechange, double lanechange, and j-turn maneuvers for uncontrolled, PID, and optimal LQR controllers in Figs 7.

As shown in Figs. 7, vehicle without controller cannot follow desired path properly and in some maneuvers losses stability and critical handling situation accurse. Whilst, additional of controller improves stability and vehicle can track desired path with minimal deviation. Also, results depict that designed controllers are adaptive to various maneuvers, whereas optimal controller performance is better than PID one. In the next stage vehicle state variation during standard lanechange maneuver has been illustrated in Figs. 8, for side slip angle, lateral velocity, acceleration, and deviation respectively.

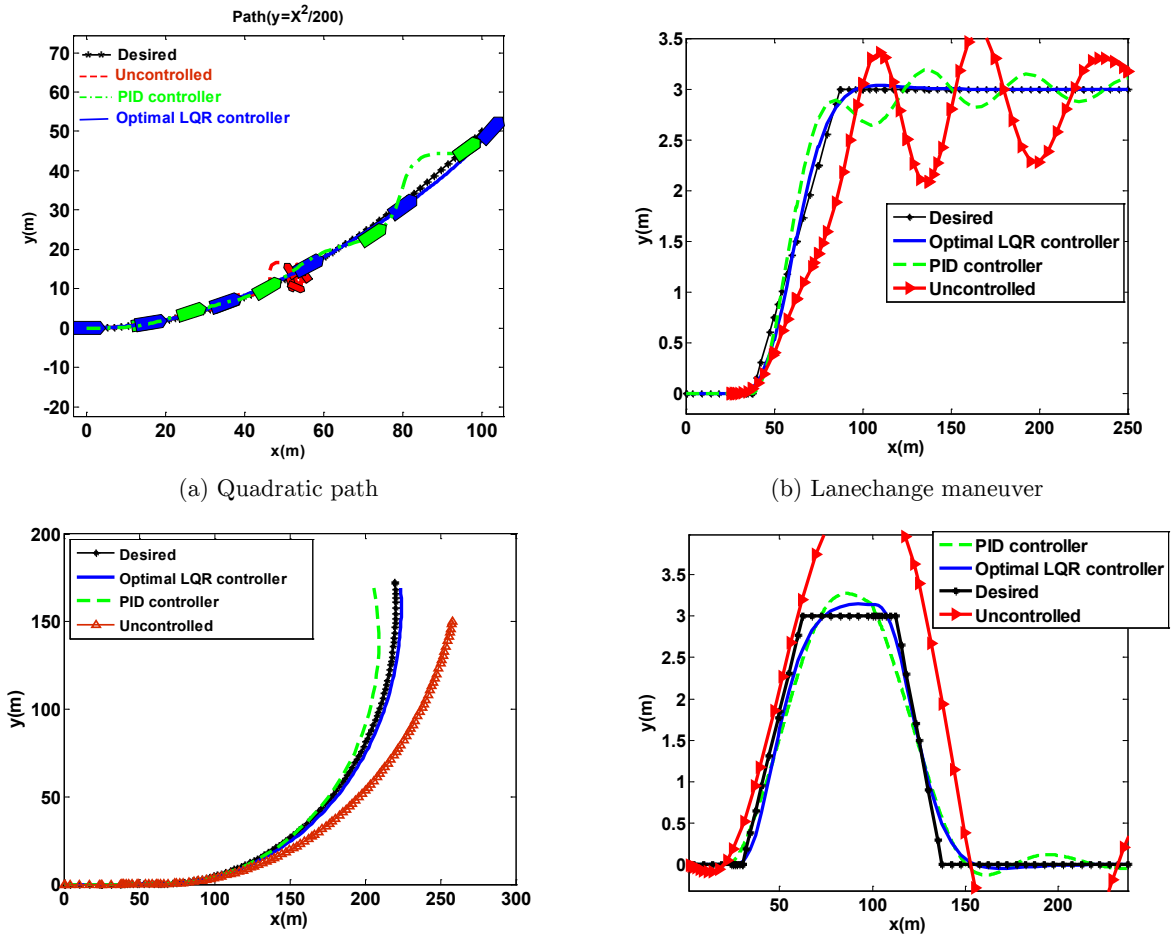

(a) Quadratic path

(b) Lanechange maneuver

(c) J-turn maneuver

(d) Double lanechage maneuver

Figure 7: Path following during various: (a) Quadratic path. (b) Lanechange. (c) J-turn. (d) Double lanechage.

Compared results indicate that, optimal LQR controller improves vehicle handling conditions. Lateral velocity and acceleration always remains below the critical margins (1 m/s and 0.8 m/s^2) [29]. So, vehicle can track desired path with minimum deviation with maintain stability and steerability. In order to analyze the controller performance control efforts (external yaw moment and corrective steer angle) are compared for PID and optimal LQR controller in Figs. 9 and 10, respectively. It is obvious that PID controller needs more control efforts, which results in extra work load on driver/vehicle model. Whereas, optimal LQR controller minimizes external yaw moment and corrective steering angle.

4.3 Obstacle avoidance

In order to enhance the effects of the controls under more severe maneuvering conditions, the single lane change test with obstacle in path with LQR and PID controllers is executed. This can be utilized to make a more intelligent choice with consideration of driver model preview distance. Simulation results for lane change maneuver with obstacle in straight part of lane change (5th second), at a constant speed of 15 m/s are shown in Figs. 8.

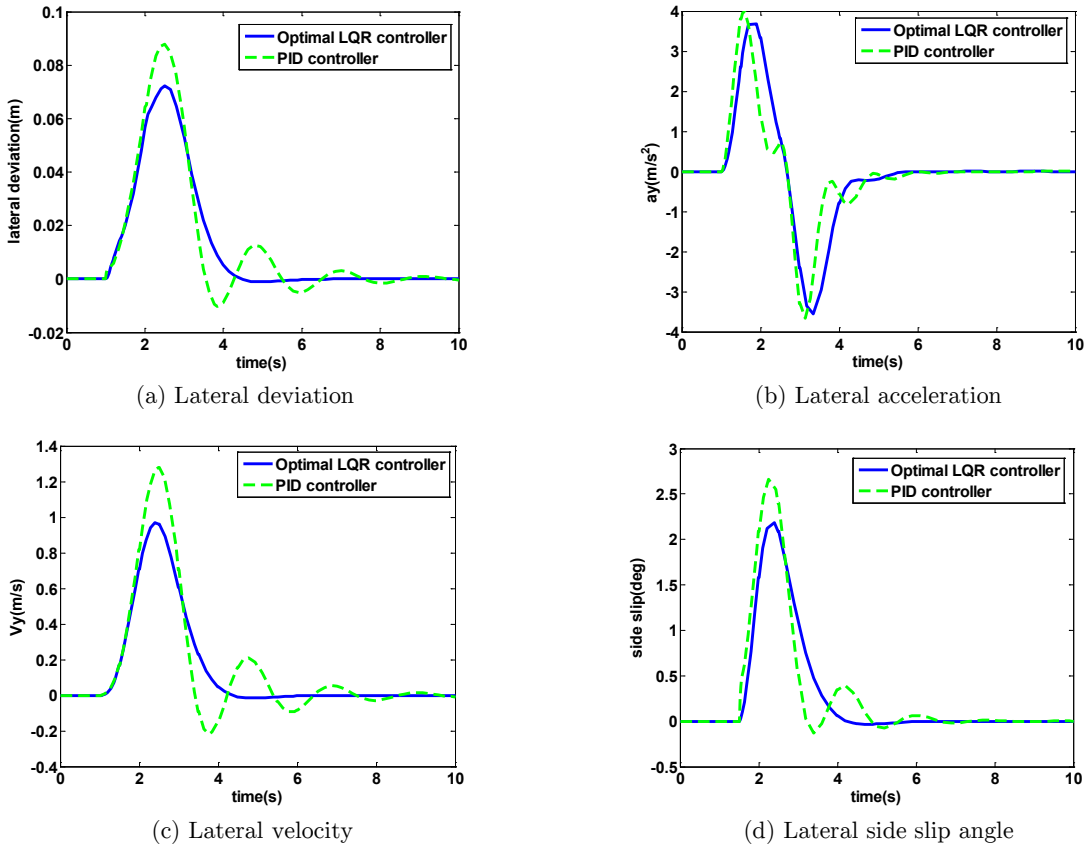

(a) Lateral deviation

(b) Lateral acceleration

(c) Lateral velocity

(d) Lateral side slip angle

Figure 8: Vehicle states over lanechange maneuver.

As shown in Figs. 11 LQR controller could follow desired path with preview of upcoming road profile. This can be utilized to make a more intelligent choice with consideration of driver model look-ahead distance obstacle avoidance and stability maintaining, even though lateral acceleration and velocity has undulation because of instantaneous steering. Optimal controller stabilize the vehicle states properly after disturbances, which makes vehicle steerable and stable after severe steering conditions.

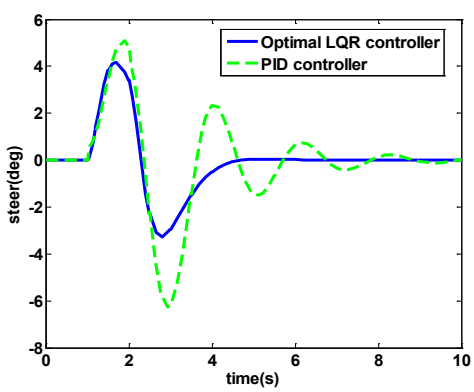

Figure 9: Steering angle during lanechange maneuver.

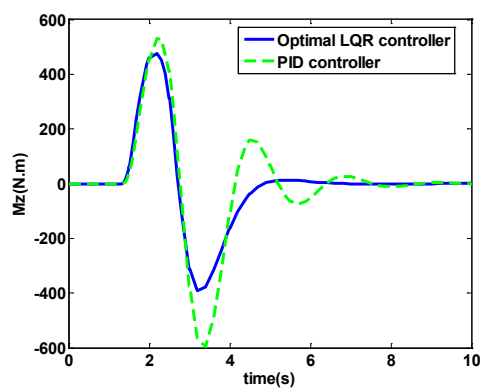

Figure 10: Yaw moment during lanechange maneuver.

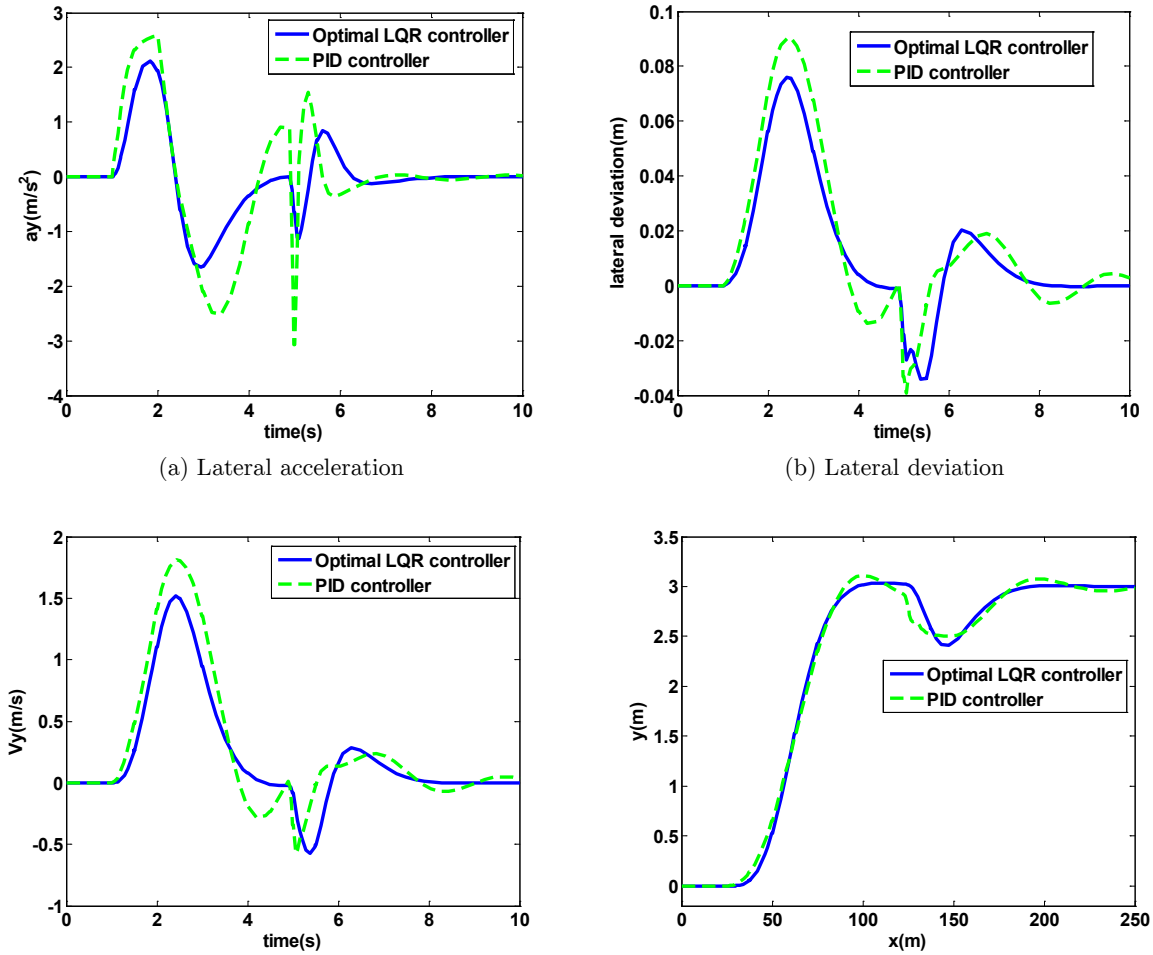

(a) Lateral acceleration

(b) Lateral deviation

(c) Lateral velocity

(d) Vehicle path

Figure 11: Simulation result comparison during lane change maneuver with quick obstacle avoidance.

5 CONCLUSION

This paper presented the comprehensive dynamic model for vehicle path following and improving its handling properties. An integrated vehicle safety control strategy for vehicle longitudinal and lateral stability was designed to optimally maintain steerabilty and stability of vehicle under different scenarios with minimizing control efforts. So, the effectiveness of integrated direct yaw moment control and corrective steering angle with optimal LQR and PID approaches evaluated in the closed-loop driver/vehicle system, for path following. The proposed control law was developed based on tracking vehicle parameters (yaw and lateral velocities) in related to previewed path by driver (lateral deviation). Controller applied corrective steering angle and direct yaw moment to maintain vehicle stability and improving maneuverability. For this purpose, a number of simulations were conducted on an 8-DOF nonlinear driver/vehicle closed-loop model for a various maneuvers. Simulation results clarified that the closed-loop driver vehicle response was stable even under severe maneuvers, in which an uncontrolled vehicle is unstable.

References

Abe, M., (1999). Vehicle dynamics and control for improving handling and active safety: from four-wheel steering to direct yaw moment control. Proc. Inst. Mech. Eng., Part K: J. Multi-body Dynam. 213 (2): 87–101.

Abe, M., (2009). Vehicle Handling Dynamics: Theory and Application. Elsevier, Oxford, UK.

Alonso, L., Perez-Oria, J., Al-Hadithi, B.M., Jimenez, A., (2013). Self-tuning PID controller for autonomous car tracking in urban traffic. System Theory, Control and Computing (ICSTCC), 17th International Conference, Sinaia, pp. 15-20.

Chu, L., Gao, X., Guo, J., Liu, H., Chao, L., Shang, M., (2012). Coordinated Control of Electronic Stability Program and Active Front Steering. Procedia Environmental Sciences 12, Part B: 1379–1386.

Cominos, P., Munro, N., (2002). PID controllers: recent tuning methods and design to specification. IEE Proceedings Control Theory & Applications 149: 46–53.

Doumiati, M., Sename, O., Dugard, L., Molina, J.J., Gaspar, P., Szabo, Z., (2013). Integrated vehicle dynamics control via coordination of active front steering and rear braking. European Journal of Control 19(2): 121–143.

Fiala, E., (1954). Lateral forces on rolling pneumatic tires. In Zeitschrift V.D.I. 96, vol. 29, 10, 114.

Goodarzi, A., Sabooteh, A., Esmailzadeh, E., (2006). Automatic path control based on integrated steering and external yaw-moment control. Proc. IMechE Part K: J. Multi-body Dynamics 222(2): 189-200.

Gordon, T.J., Best, M.C., Dixon, P.J., (2002). An automated driver based on convergent vector fields. Proc IMechE Part D: J. Automobile Engineering 216(4): 329–347.

Guo, J., Li, L., Li, K., Wang, R., (2013). An adaptive fuzzy-sliding lateral control strategy of automated vehicles based on vision navigation. Vehicle System Dynamics: International Journal of Vehicle Mechanics and Mobility 51(10): 1502-1517.

Horiuchi, S., Okada, K., Nohtomi, S., (1999). Improvement of vehicle handling by nonlinear integrated control of four wheel steering and four wheel torque. JSAE Review 20: 459-464.

Hwang, T.H., Park, K., Heo, S.J., Lee, S.H., Lee, J.C., (2008). Design of integrated chassis control logics for AFS and ESP. International Journal of Automotive Technology 9(1): 17-27.

Jinlai, M., Bofu, W., Jie, C., (2011). Comparisons of 4WS and Brake-FAS based on IMC for vehicle stability control. Journal of Mechanical Science and Technology 25(5): 1265-1277.

Kang, J., Hindiyeh, R.Y., Moon, S.W., Gerdes, J.C., Yi, K., (2008). Design and Testing of a Controller for Autonomous Vehicle Path Tracking Using GPS/INS Sensors. Proceedings of the 17th World Congress The International Federation of Automatic Control Seoul, Korea, 2093-2098.

Kazemi, R., Hamedi, B., Javadi, B., (2000). A new sliding mode controller for four-wheel anti-lock braking system (ABS). SAE Automotive Dynamics & Stability Conference, paper Num. 2000-01-1639, 2000.

Kirk, D.E., (2004). Optimal Control Theory: An Introduction. Dover Publication, Mineola, N.Y.

Mashadi, B., Mahmoodi, M., Ahmadizadeh, P., Oveisi, A., (2014). A path-following driver/vehicle model with optimized lateral dynamic controller. Latin American journal of solids and structures 11(4): 613-630.

Mashadi, B., Mahmoodi, M., Kakae, A.H., Hoseini, R. (2013). Vehicle path following in the presence of driver inputs. Proceedings of the Institution of Mechanical Engineers, Part K: Journal of Multi-body Dynamics 227(2): 115-132.

Mashadi, B., Majidi, M., (2014). Global Optimal Path Planning of An Autonomous Vehicle for Overtaking a Moving Obstacle. Latin American journal of solids and structures 11(10): 2555-2572.

Mirzaei, M., (2010). A new strategy for minimum usage of external yaw moment in vehicle dynamic control system. Transportation Research Part C: Emerging Technologies 18(2): 213–224.

Mirzaeinejad, H., Mirzaei, M., (2010a). A new approach for modeling and control of two-wheel antilock brake systems. Proc. IMechE, Part K: J. Multi-body Dynamics 225: 179-192.

Mirzaeinejad, H., Mirzaei, M., (2010b). A novel method for non-linear control of wheel slip in anti-lock braking systems. Control Engineering Practice 18(8): 918-926.

Moon, C., Choi, S.B., (2011). A driver model for vehicle lateral dynamics. Int. J. Vehicle Design 56(1,2,3,4): 49-80.

Selby, M., Manning, W.J., Brown, M.D., Crolla, D.A., (2001). A Coordination Approach for DYC and Active Front Steering. SAE Technical Paper 2001-01-1275, 2001.

Shuai, Z., Zhang, H., Wang, J., Li, J., Ouyang, M., (2014). Lateral motion control for four-wheel-independent-drive electric vehicles using optimal torque allocation and dynamic message priority scheduling. Control Engineering Practice 24: 55–66.

Silva, J.E., Sousa, J.B., (2014). A Dynamic Programming Based Path-Following Controller for Autonomous Vehicles. Control and Intelligent Systems 39(4): 245-253.

Tchamna, R., Youn, I., (2013). Yaw rate and side-slip control considering vehicle longitudinal dynamics International. Journal of Automotive Technology 14(1): 53-60.

Vahedi, M., Hasheminejad, S.M., Hoshangi, A., (2014). Active Vibration Control of An Arbitrary Thick Piezo-laminated Beam with Imperfectly Integrated Sensor and Actuator Layers. Latin American journal of solids and structures 11(4): 1957-1982.

Wei, Z., Guizhen, Y., Jian, W., Tianshu, S., Xiangyang, X., (2009). Self-Tuning Fuzzy PID Applied to Direct Yaw Moment Control For Vehicle Stability. The Ninth International Conference on Electronic Measurement & Instruments.

Wu, J., Wang, Q., Wei, X., Tang, H., (2010). Studies on improving vehicle handling and lane keeping performance of closed-loop driver–vehicle system with integrated chassis control. Mathematics and Computers in Simulation 80(12): 2297–2308.

Yamakado, M., Takahashi, J., Saito, S., (2012). Comparison and combination of direct yaw-moment control and G-Vectoring control. Vehicle System Dynamics 50(1): 111-130.

Yang, X., Wang, Z., Peng, W., (2009). Coordinated control of AFS and DYC for vehicle handling and stability based on optimal guaranteed cost theory. Vehicle System Dynamics 47(1): 57–79.